

Figure 7. ^{129}Xe CP/MAS spectrum (a) same sample as described in Figure 6b, and (b) same sample as described in Figure 6c.

both singly and doubly occupied by xenon are indicated.

^{13}C NMR spectra for these two samples and for samples recrystallized from octane and dodecane (empty host lattice) are shown in Figure 6 (parts a–c). The C_{18} methyl carbon appears to be especially sensitive to the presence or absence of guest or to the nature of the guest. This is thought to originate in the flexibility of the ring to which the C_{18} methyl is attached. The line marked C_{18} in Figure 6a corresponds to the empty host lattice. C_{18}' and C_{18}'' then correspond to cages filled or half-filled with xenon, and C_{18}''' corresponds to cages filled with octane. The C_{19} line also is sensitive to the presence of octane. This appears to be the general case for guests occupying the neck of the cage.

The lines due to C_{13} and C_{15} also show some sensitivity to the presence of guest molecules. The shift of these two carbons, being ortho to the phenolic hydroxyl group, is sensitive to the torsional angle of the OH group with respect to the plane of the aromatic ring. The torsional angle may well change depending on the cage

content. Indeed, for the empty host lattice (Figure 6a) there appears to be some structure on the C_{13} , C_{15} lines and C_{18} as well. These features suggest the presence of some disorder in the empty lattice, related to rotation or movement of flexible parts of the host lattice molecules so as to partially occupy the empty cage space.

The lines due to enclathrated octane, labeled 1–4 in Figure 6d occur at 13.2, 19.4, 28.2, and 23.7 ppm. These positions are quite different from those measured in solution 13.9, 22.9, 32.2, and 29.5 ppm.²⁶ This can be explained by the fact that octane in the Dianin's compound cage is not in the extended all-trans configuration. X-ray diffraction has shown that the end methyl group of enclathrated *n*-heptanol, a molecule of similar length as octane, is gauche with respect to the C_4 methylene group. This conformer is considerably shorter than the all-trans form which cannot fit in the Dianin's compound cage. The same must be true for octane: rotation of the end methyl groups by 120° about the C_2 – C_3 bond allows the incorporation of octane in the clathrate cage.

The presence of both xenon and octane as guests gives rise to a small shift in the octane carbon resonances, visible mainly as line broadening except for C_4 where two lines are partially resolved. Evidently the presence of two guests causes short-range disorder not only for the host lattice but also for guests in neighboring cages.

It is also clear from the ^{13}C and ^{129}Xe spectra that in no case is there evidence for clustering; i.e., cages with two Xe atoms per cage are not favored over cages containing a single Xe atom. One cannot expect exact statistical distributions of empty, half full, and completely full cages, as the samples were not prepared under equilibrium conditions.

Supplementary Material Available: Tables of atomic parameters and anisotropic temperature factors and a conversion chart of the numbering for Dianin's compound atoms (3 pages); table of observed and calculated structure factors (17 pages). Ordering information is given on any current masthead page.

Separation by ^{23}Na NMR of the Unimolecular and Bimolecular Components of the Dissociation Kinetics of 18-Crown-6- Na^+ in Some Nonaqueous Solvents

Helen P. Graves and Christian Detellier*

Contribution from the Ottawa-Carleton Chemistry Institute, Ottawa University Campus, Ottawa, Ontario K1N 9B4, Canada. Received December 29, 1987

Abstract: The kinetics of dissociation of (18-crown-6, Na^+)¹ in propylene carbonate (PC), acetonitrile (AN), pyridine (PY), and acetone (AC) have been determined by ^{23}Na NMR. Two mechanisms of exchange, namely unimolecular dissociative and bimolecular, have been shown to be in competition in the first three solvents. In acetone, the exchange mechanism is almost exclusively unimolecular. The activation parameters for the unimolecular exchange have been determined in all four solvents. $\Delta H_{\text{uni}}^{\ddagger}$ follows the trend $\text{AN} < \text{AC} < \text{PY} \approx \text{PC}$. A compensation effect between ΔH^{\ddagger} and ΔS^{\ddagger} was observed. As a result, $\Delta G_{300\text{K}}^{\ddagger}$ is in the range 50–58 $\text{kJ}\cdot\text{mol}^{-1}$ (AC and PY, respectively). No direct relationship between the Gutmann donicity number and ΔG^{\ddagger} or ΔH^{\ddagger} could be established, showing that several factors, including conformational rearrangement of the ligand and reorganization of the solvent cage, contribute to the barrier of exchange. The activation parameters were also determined for the bimolecular exchange mechanism in PC: $\Delta H_{\text{bi}}^{\ddagger} = 35 \pm 1 \text{ kJ}\cdot\text{mol}^{-1}$ and $\Delta S_{\text{bi}}^{\ddagger} = -16 \pm 3 \text{ J}\cdot\text{K}^{-1}\cdot\text{mol}^{-1}$.

The recognition of cations by macrocyclic hosts is well documented.² However, the factors responsible for the recognition are far from being well understood, particularly the role of the

solvent. There are only a few studies in the literature which deal with the kinetics of the crown ether–alkali metal cation association/dissociation processes.^{3–15} Since the rate of formation of

(1) 18-Crown-6 (18C6): 1,4,7,10,13,16-hexaoxacyclooctadecane.
 (2) (a) Sutherland, I. O. *J. Chem. Soc., Faraday Trans. 1* **1986**, *82*, 1145–1159. (b) Lehn, J.-M. *Science (Washington, D.C.)* **1985**, *227*, 849–856. (c) Takeda, Y. In *Host–Guest Complex Chemistry III*; Vögtle, F., Weber, E., Eds.; 1984; Vol. 121, pp 1–38. (d) Hilgenfeld, R.; Saenger, W. In *Host–Guest Complex Chemistry II*; Vögtle, F., Ed.; 1982; Vol. 101, pp 1–82. (e) *Host–Guest Complex Chemistry I*; Vögtle, F., Ed.; 1981; Vol. 98.

(3) (a) Shchori, E.; Jagur-Grodzinski, J.; Luz, Z.; Shporer, M. *J. Am. Chem. Soc.* **1971**, *93*, 7133–7138. (b) Shchori, E.; Jagur-Grodzinski, J.; Shporer, M. *J. Am. Chem. Soc.* **1973**, *95*, 3842–3846.
 (4) Shporer, M.; Luz, Z. *J. Am. Chem. Soc.* **1975**, *97*, 665–666.
 (5) (a) Mei, E.; Popov, A. I.; Dye, J. L. *J. Phys. Chem.* **1977**, *81*, 1677–1681. (b) Mei, E.; Dye, J. L.; Popov, A. I. *J. Am. Chem. Soc.* **1977**, *99*, 5308–5311.

Table I. ^{23}Na NMR Characteristics of (18C6- Na^+) in Various Solvents

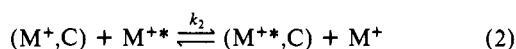
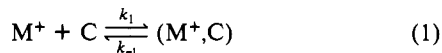
solvent ^a	DN ^b	ϵ^c	η^e (mP)	δ (Na^+, C) ^f (ppm)	$\Delta\delta^g$ (Hz)	T_1^{-1} ^h (Hz)	$(k_A + k_B)\text{lim}^i$ (s^{-1})
NM	2.7	35.9 ^d	6.14	-16.3	121	332	3.4×10^3
AN	14.1	36.0	3.41	-14.9	590	73.0	2.6×10^5
PC	15.1	64.9	25.3	-16.2	475	297	3.7×10^4
AC	17.0	20.6	3.03	-15.8	600	82.0	2.1×10^5
PY	33.1	12.9	8.84	-12.4	1080	1280	8.2×10^4

^aNM = nitromethane; AN = acetonitrile; PC = propylene carbonate; AC = acetone; PY = pyridine. ^bGutmann donicity number, from ref 26. ^cDielectric constant at 298 K, unless otherwise stated. From ref 24. ^d303 K. ^eViscosities at 298 K, from ref 24. ^f ^{23}Na chemical shift of (Na^+ , 18C6) referenced to $^{23}\text{NaCl}$ 0.1 M in water and corrected for bulk magnetic susceptibility. [Na^+ , 18C6] = 20 mM; anion, BPh_4^- ; $T = 301.5$ K. Our data is in good agreement with ref 22. ^g ^{23}Na chemical shift difference (in Hz, at 79.35 MHz) between solvated Na^+ and (Na^+ , 18C6). Same conditions as f. ^h ^{23}Na longitudinal relaxation time of (Na^+ , 18C6). ⁱHighest detectable values of $(k_A + k_B)$ for $\nu_0 = 79.35$ MHz (see eq 5 and text).

complexes between alkali metal cations and crown ethers or cryptands in nonaqueous solution is generally diffusion-controlled,¹⁶ the rate of dissociation, which is responsible for the selectivity, is in a range ideally suited for study by alkali metal cation NMR,¹⁷ notably ^{23}Na ,^{3,8-14} ^{39}K ,^{4,6} and ^{133}Cs .^{5,7}

The kinetics of complexation have been studied by ultrasonic techniques,¹⁵ and, generally, the Eigen-Winkler multistep mechanism accounts for the ultrasonic data.¹⁵

NMR results⁶⁻¹¹ have shown that two mechanisms, namely unimolecular dissociative (eq 1) and bimolecular interchange (eq 2), have to be considered when describing the exchange between complexed (M^+, C) and solvated cation (M^+).



The dissociative mechanism was assumed to be dominant in early studies on Cs^+ -18C6 in pyridine^{5b} and propylene carbonate.^{5a} The bimolecular exchange process was shown to be dominant in the case of K^+ -18C6 in several nonaqueous media.⁶ Both mechanisms are operative for (Na^+ -18C6) in tetrahydrofuran, depending upon the nature of the associated anion.^{8a} Particularly, the thiocyanate anion was shown to strongly favor the bimolecular exchange mechanism.^{8a} Very recently, the activation parameters for the dissociation process of (18C6- Na^+) in acetone, methanol, and pyridine have been published.¹² Despite the nature of the anion (thiocyanate) and the high concentration (0.1 M), the unimolecular dissociative mechanism was reported to be predominant.¹²

Since, as it was mentioned previously by Popov et al.^{7a} "it is

(6) Schmidt, E.; Popov, A. I. *J. Am. Chem. Soc.* **1983**, *105*, 1873-1878.

(7) (a) Strasser, B. O.; Shamsipur, M.; Popov, A. I. *J. Phys. Chem.* **1985**, *89*, 4822-4824. (b) Shamsipur, M.; Popov, A. I. *J. Phys. Chem.* **1987**, *91*, 447-451.

(8) (a) Strasser, B. O.; Hallenga, K.; Popov, A. I. *J. Am. Chem. Soc.* **1985**, *107*, 789-792. (b) Strasser, B. O.; Popov, A. I. *J. Am. Chem. Soc.* **1985**, *107*, 7921-7924. (c) Szczygiel, P.; Shamsipur, M.; Hallenga, K.; Popov, A. I. *J. Phys. Chem.* **1987**, *91*, 1252-1255.

(9) (a) Stöver, H. D. H.; Delville, A.; Detellier, C. *J. Am. Chem. Soc.* **1985**, *107*, 4167-4171. (b) Delville, A.; Stöver, H. D. H.; Detellier, C. *J. Am. Chem. Soc.* **1985**, *107*, 4172-4175.

(10) Delville, A.; Stöver, H. D. H.; Detellier, C. *J. Am. Chem. Soc.* **1987**, *109*, 7293-7301.

(11) Brière, K.; Detellier, C. *J. Phys. Chem.* **1987**, *91*, 6097-6099.

(12) Lincoln, S. F.; White, A.; Hounslow, A. M. *J. Chem. Soc., Faraday Trans. 1* **1987**, *83*, 2459-2466.

(13) Amat, E.; Cox, B. G.; Schneider, H. *J. Magn. Reson.* **1987**, *71*, 259-270.

(14) Phillips, R. C.; Khazaali, S.; Dye, J. L. *J. Phys. Chem.* **1985**, *89*, 606-612.

(15) (a) Gokel, G. W.; Echegoyen, L.; Kim, M. S.; Eyring, E. M.; Petrucci, S. *Biophys. Chem.* **1987**, *26*, 225-233. (b) Maynard, K. J.; Irish, D. E.; Eyring, E. M.; Petrucci, S. *J. Phys. Chem.* **1984**, *88*, 729-736. (c) Chen, C.; Wallace, W.; Eyring, E. M.; Petrucci, S. *J. Phys. Chem.* **1984**, *88*, 2541-2547. (d) Wallace, W.; Chen, C.; Eyring, E. M.; Petrucci, S. *J. Phys. Chem.* **1985**, *89*, 1357-1366.

(16) (a) Lockhart, J. C. *J. Chem. Soc., Faraday Trans. 1* **1986**, *82*, 1161-1167. (b) Cox, B. G.; Garcia-Rosas, J.; Schneider, H. *J. Am. Chem. Soc.* **1981**, *103*, 1054-1059.

(17) Detellier, C. In *NMR of Newly Accessible Nuclei*; Laszlo, P., Ed.; Academic Press: New York, 1983; Vol. 2, Chapter 5, pp 105-151.

important to investigate not only the rates of exchange involved in the complexation kinetics of crown ethers but also the mechanism of exchange", and since we have shown previously⁹⁻¹¹ that a systematic study of the experimental rate constants as a function of both cation and crown concentration leads to the possible separation of the two mechanisms, we have applied that approach to the (18C6- NaBPh_4) system in acetonitrile, acetone, pyridine, and propylene carbonate.

Experimental Section

18-Crown-6 (Aldrich, 99%) was purified following the procedure described by Gokel et al.¹⁸ and vacuum dried over P_2O_5 for a minimum of 24 h, at 50 °C. The complete removal of acetonitrile from the recrystallized crown was confirmed by ^1H NMR. Sodium tetraphenylborate (Aldrich 99+%, ACS reagent) was recrystallized from cyclohexane with a minimal amount of ethanol and vacuum dried over P_2O_5 for at least 24 h at 50 °C prior to use. Pyridine (PY) (BDH assured), acetonitrile (AN) (BDH assured), acetone (AC) (Fisher 99.5%, Spectranalyzed), and nitromethane (NM) (Aldrich 96%, Gold Label) were dried under reflux, over calcium hydride for at least 2 h, distilled under nitrogen, and stored under argon. Propylene carbonate (PC) (Burdick & Jackson, water content 0.012%) was dried over molecular sieves 4 Å. All the spectra were recorded within 48 h of the preparation of the samples. NMR tubes were sealed with Parafilm under argon.

^{23}Na NMR spectra were obtained as described previously^{9,10} on a Varian XL-300 spectrometer, at 79.35 MHz; 90° pulse widths were typically 17 μs (PC), 27 μs (PY), 31 μs (AC), 24 μs (NM), and 31 μs (AN). They were systematically measured before each set of experiments. T_1 , T_2 , and temperature measurements were done as described previously.^{9,10} The temperature of the sample was deemed to be reliable to ± 0.5 K. The signal to noise ratio was always at least 100. The chemical shifts were referenced to $^{23}\text{NaCl}$ 0.1 M in water and were corrected for bulk magnetic susceptibility. In the case of PC, the correction was done from the measurement of ^{23}Na chemical shifts in two different field geometries on a Varian XL-300 and a Varian FT-80.

The errors on $(k_A + k_B)$ reported in Table II were obtained from the experimental errors on T_2^{-1} and T_1^{-1} , in the case of the moderately rapid exchange (eq 5). A full line shape analysis for two-site exchange¹⁹ using a Simplex fitting procedure²⁰ was used to derive the pseudo-first-order rate constants for non-Lorentzian line shapes. In that case, the errors were estimated from the rms of the regression. The errors on k_{-1} and k_2 are the standard deviations on the slope and the Y-intercept of the linear regressions of $(k_A + k_B)$ as a function of $(1 - \rho)^{-1}$ (see Figures 3, 4, and 5). Similarly, the errors on ΔH^\ddagger and ΔS^\ddagger are the standard deviations of the linear regressions on the Eyring plots (Figure 6). The errors on ΔG^\ddagger have been calculated from the corresponding errors on k_{-1} and k_2 at 301.5 K.²¹

Results

Titration curves of $^{23}\text{NaBPh}_4$ by 18-crown-6 were done in five nonaqueous solvents: nitromethane (NM), acetonitrile (AN), propylene carbonate (PC), acetone (AC), and pyridine (PY). The donicity numbers, dielectric constants, and viscosities of these solvents are given in Table I.

^{23}Na chemical shifts, transverse and longitudinal relaxation rates, all point to the evidence of the formation of a unique 1:1 18C6: Na^+ complex, whose formation constant is $>10^4$. Our

(18) Gokel, G. W.; Cram, D. J.; Liotta, C. L.; Harris, H. P.; Cook, F. L. *Org. Synth.* **1977**, *57*, 30-33.

(19) Sandström, J. *Dynamic NMR Spectroscopy*; Academic Press: New York, 1982.

(20) Deming, S. N.; Morgan, S. S. *Anal. Chem.* **1973**, *45A*, 278-282.

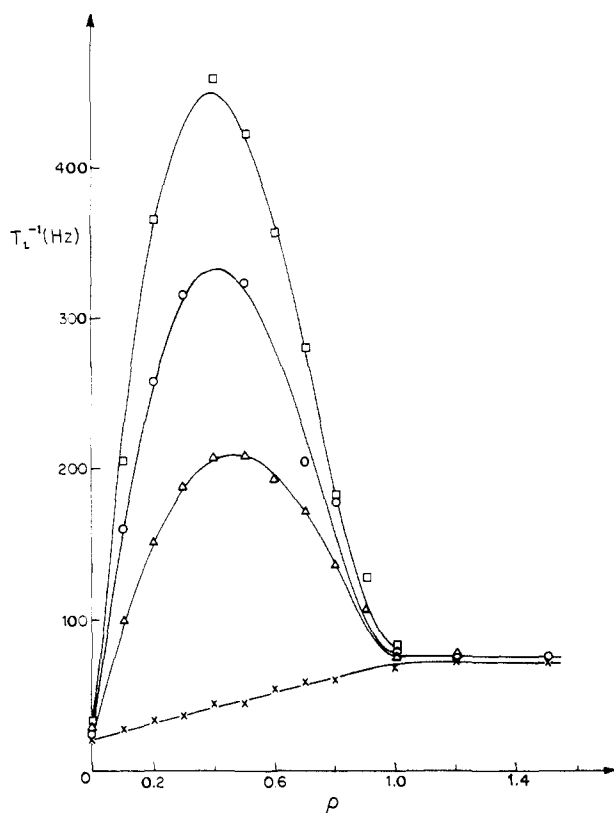


Figure 1. ²³Na transverse (Δ , \circ , \square) and longitudinal (\times) relaxation rates of sodium tetraphenylborate in acetonitrile as a function of $\rho = [18C6]/[NaBPh_4]$. $[NaBPh_4] = 5.0$ mM (\square), 20 mM (\circ , \times), and 50 mM (Δ). $T = 295$ K. The data points are experimental, and the curves are calculated from the values of k_{-1} and k_2 obtained from eq 6 and given in Table II.

chemical shift data agree with the chemical shifts variations previously published by Lin and Popov.²² The values of the characteristic chemical shifts of the complex are given in Table I. They are in a small range (-14.9 to -16.3 ppm), except for pyridine in which the ²³Na⁺ resonance appears at -12.4 ppm. For acetonitrile, Figure 1 shows the ²³Na longitudinal relaxation rate which parallels the chemical shift variation. This is not the case for the transverse relaxation rate. A strong increase is observed for $0 < \rho = [18C6]/[Na^+] < 1$. For example, at $[Na^+] = 5.0 \times 10^{-3}$ M, T_2^{-1} increases from 30 ($\rho = 0$) to 450 Hz ($\rho = 0.4$). For $\rho > 1$, T_1^{-1} and T_2^{-1} are almost identical, the difference being the inhomogeneity contribution to T_2^{-1} ($T_{2,inh}^{-1}$). This behavior is characteristic of a moderately rapid exchange for which the transverse relaxation rate contains an exchange contribution when the longitudinal relaxation rate is unaffected by the exchange^{9,23} (eq 3). A bimolecular contribution to the exchange can be immediately detected, since the transverse relaxation rates are strongly dependent on the total sodium concentration (see below).

$$T_{2,obsd}^{-1} = T_1^{-1} + T_{2,inh}^{-1} + T_{2,ex}^{-1} \quad (3)$$

Figure 2 shows the ²³Na transverse and longitudinal relaxation rates for acetone and propylene carbonate as a function of ρ . These two solvents are characterized by very different viscosities, 3.03 and 25.3 mP, respectively, at 298 K.²⁴ Viscosity is the factor responsible for the order of magnitude of the relaxation rates: from 30 to 200 Hz for AC and from 200 to 400 Hz for PC. The increase in T_1^{-1} from 30 (solvated Na⁺) to 80 Hz (complexed Na⁺) in AC and from 200 to 300 Hz in PC is due to the increase in

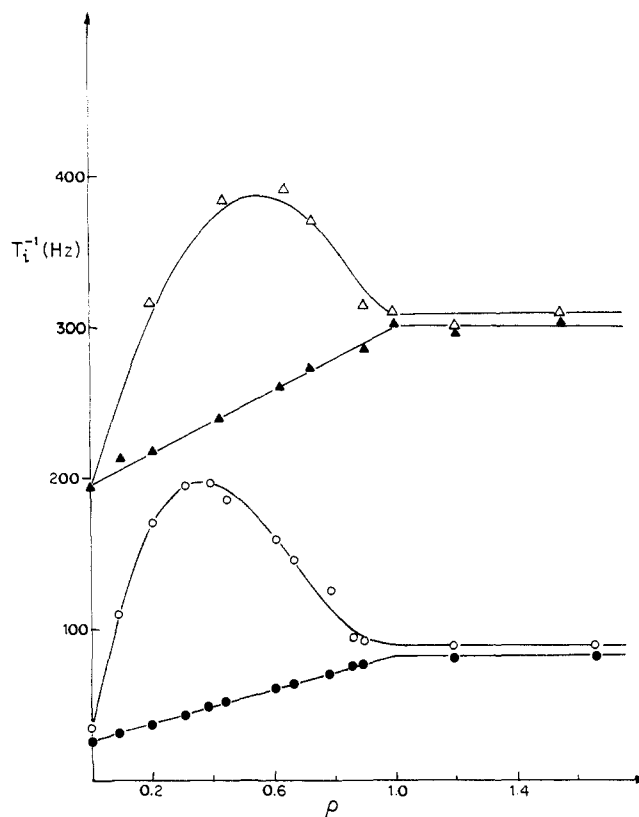


Figure 2. ²³Na transverse (Δ , \circ) and longitudinal (\blacktriangle , \bullet) relaxation rates of sodium tetraphenylborate in acetone (\circ , \bullet) and propylene carbonate (Δ , \blacktriangle) as a function of $\rho = [18C6]/[NaBPh_4]$. $[NaBPh_4] = 20$ mM. $T = 301.5$ K. The data points are experimental, and the curves are calculated from the values of k_{-1} and k_2 obtained from eq 6 and given in Table II.

the quadrupole coupling constant (χ) in going from the solvated sodium to a more dissymmetric species.²⁵ Finally, the transverse relaxation rate contains an exchange contribution which has the same order of magnitude in both systems. Since the shapes of the relationships between T_2^{-1} and ρ are different, the exchange mechanism must be different in the two solvents (see below).

We are in the presence of a two-site uncoupled spin system shown in eq 4. "A" represents solvated sodium, and "B" represents complexed sodium.



Equation 5 relates the exchange contribution, $T_{2,ex}^{-1}$, to the lifetime of sodium in the two sites, $\tau = (k_A + k_B)^{-1}$, under the condition of moderately fast exchange.^{9-11,23} ($k_A + k_B$) could

$$T_{2,ex}^{-1} = 4P_A P_B \pi^2 (\nu_A - \nu_B)^2 (k_A + k_B)^{-1} \quad (5)$$

be calculated from eq 3 and 5. When non-Lorentzian line shapes were obtained, which was the case for PY at all the temperatures and for AN, AC, and PC at lower temperatures, $(k_A + k_B) = \tau^{-1}$ was calculated from a complete line shape analysis (see Experimental Section). This pseudo-first-order rate constant could be related to both k_{-1} (eq 1) and k_2 (eq 2) as shown in eq 6.⁹⁻¹¹

$$k_A + k_B = k_{-1}(1 - \rho)^{-1} + k_2[Na^+]_T \quad (6)$$

From this equation, one could expect a linear relationship between $k_A + k_B$ and $(1 - \rho)^{-1}$ for a given total sodium concentration ($[Na^+]_T$). This is indeed observed in Figures 3, 4, and 5, respectively, for AN, AC, and PC at various temperatures. k_{-1} is given directly from the slope of these linear relationships and k_2 from their Y-intercept. It is interesting also to note that, in

(21) Reference 19, p 109.
 (22) Lin, J. D.; Popov, A. I. *J. Am. Chem. Soc.* **1981**, *103*, 3773-3777.
 (23) Woessner, D. E. *J. Chem. Phys.* **1961**, *35*, 41-48.
 (24) "Organic Solvents", 4th ed; Riddick, J. A.; Bunger, W. B.; Sakano, T. K. In *Techniques of Chemistry*, Vol. II; Weissberger, A., Ed.; Wiley-Interscience, John Wiley and Sons: New York, 1986.

(25) (a) Detellier, C.; Robillard, M. *Can. J. Chem.* **1987**, *65*, 1684-1687.
 (b) Bisnaire, M.; Detellier, C.; Nadon, D. *Can. J. Chem.* **1982**, *60*, 3071-3076.

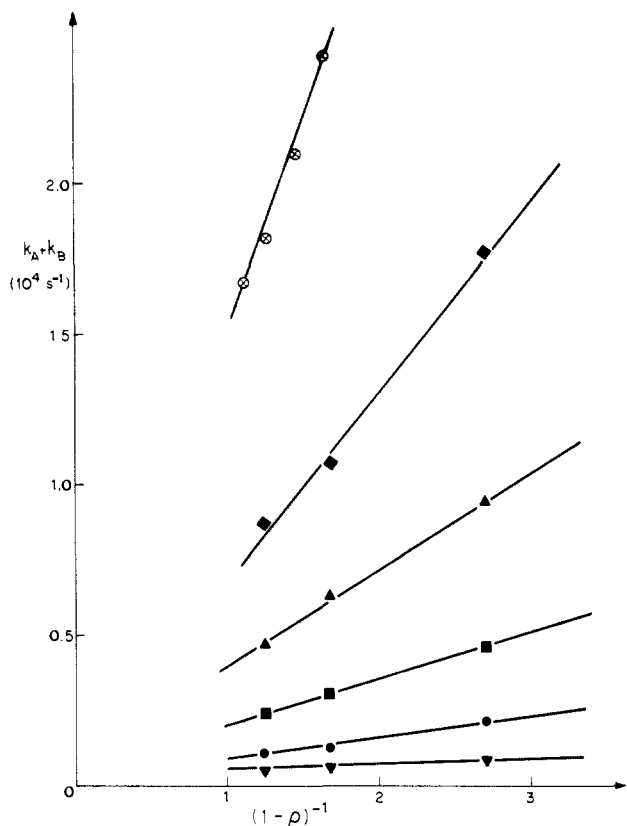


Figure 3. Pseudo-first-order rate constants ($k_A + k_B$; see eq 4 and 5) for the exchange of $^{23}\text{Na}^+$ between two sites (solvated and complexed sodium) in acetone, as a function of $(1 - \rho)^{-1}$ (see eq 6) at six different temperatures: (∇), 249.4; (\bullet), 258.8; (\blacksquare), 268.8; (\blacktriangle), 279.2; (\blacklozenge), 288.2; (\odot), 301.5 K; $[\text{NaBPh}_4] = 20 \text{ mM}$.

the case of a moderately rapid exchange, when Lorentzian line shapes are observed and eq 5 applies, k_{-1} and k_2 can be obtained from a two-parameter nonlinear regression on the $T_2^{-1} - \rho$ relationship. Figures 1 and 2 show the results of such a nonlinear regression analysis. The results are identical with those obtained from the linear relationships of Figures 3–5. Figure 3 (AC) shows a typical unimolecular decomplexation mechanism (eq 1) since there is a convergence of all the linear relationships to the origin. As the temperature increases, there is a gradual increase of the slope, allowing the determination of the activation parameters. The Eyring plot is given on Figure 6. In the case of acetonitrile (Figure 4) there is no convergence at the origin. There is a definite bimolecular exchange component to the measured pseudo-first-order rate constant. Again, one can observe a gradual increase of k_{-1} when the temperature was increased. The Y-intercept ($k_2[\text{Na}^+]_T$) also increases with temperature, but the range of k_2 obtained and the error resulting from the extrapolation precludes any useful quantitative determination of the activation parameters for the bimolecular process. The variation of $T_{2,\text{obsd}}^{-1}$ with the total sodium concentration (Figure 1) is further indication of the presence of a bimolecular component.

Clearly, the bimolecular mechanism becomes the major one in propylene carbonate (Figure 5). Here, the relationships between $(k_A + k_B)$ and $(1 - \rho)^{-1}$ extrapolate far from the origin. In this case, both k_{-1} and k_2 can be obtained at different temperatures with enough precision to permit the determination of the activation parameters for both mechanisms. The Eyring plots are given in Figure 6.

We have shown that the mechanism of exchange is purely bimolecular for monobenzo-15-crown-5- Na^+ in nitromethane,¹¹ which is a solvent characterized by a very low donicity number (D.N. = 2.7). Unfortunately, for 18C6- Na^+ the chemical shift difference between the two sites is not large enough to have the transverse relaxation rate affected by the exchange. Limiting values for $k_A + k_B$ are given in Table I. Any pseudo-first-order

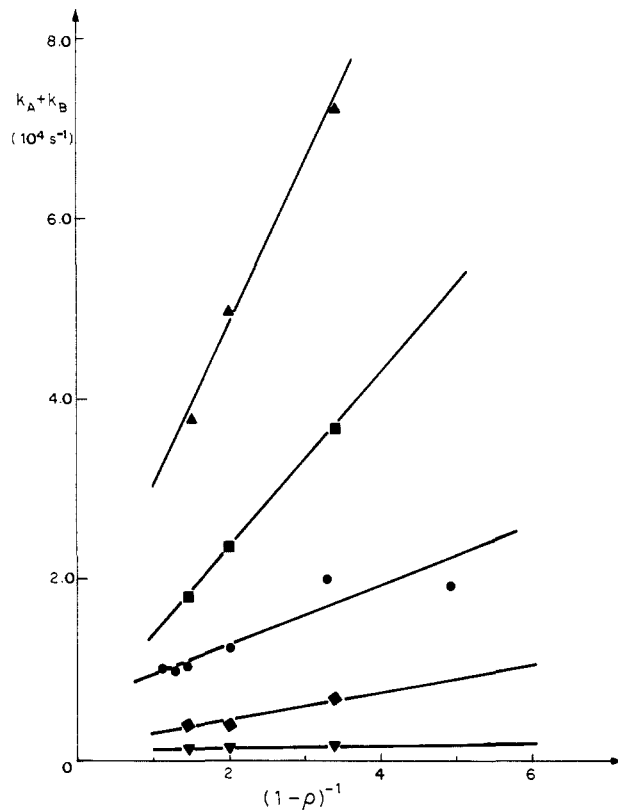


Figure 4. $(k_A + k_B)$ in acetonitrile, as a function of $(1 - \rho)^{-1}$ at these temperatures: (∇), 252.6; (\blacklozenge), 273.6; (\bullet), 295.2; (\blacksquare), 307.6; (\blacktriangle), 324.4 K. $[\text{NaBPh}_4] = 20 \text{ mM}$.

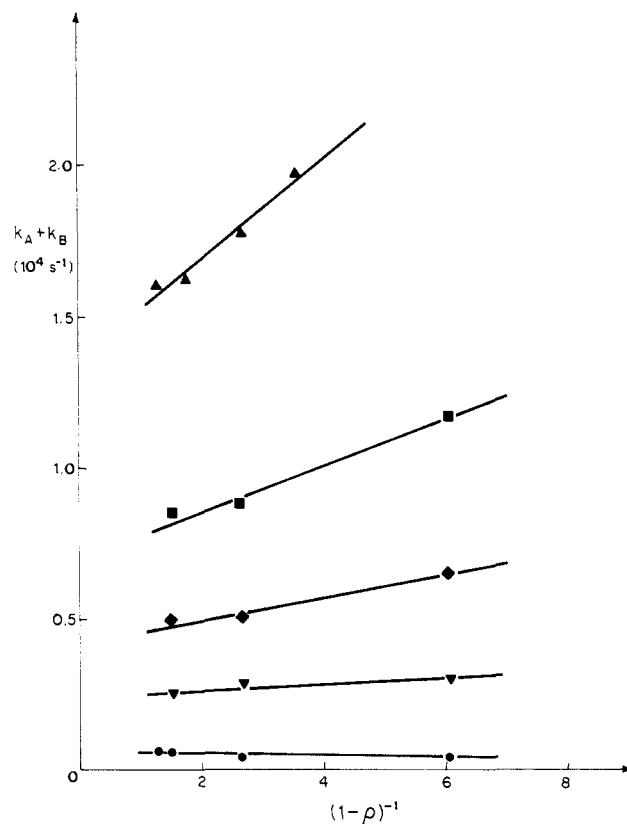


Figure 5. $(k_A + k_B)$ in propylene carbonate, as a function of $(1 - \rho)^{-1}$ at these temperatures: (\bullet), 249.4; (∇), 268.8; (\blacklozenge), 279.2; (\blacksquare), 288.2; (\blacktriangle), 301.5 K.

rate constant larger than $(k_A + k_B)_{\text{lim}}$ will not be detected under the given conditions. These limiting values were calculated from eq 5, with $T_{2,\text{ex,lim}}^{-1}$ given by $T_{2,\text{ex,lim}}^{-1} = 0.2 \times T_{1,\text{obsd}}^{-1} + T_{2,\text{inh}}^{-1}$. With

Table II. Kinetics Parameters of (18C6, Na^+) in Various Solvents

solvent ^a	$(k_A + k_B)^b$	k_{-1}^c (s ⁻¹)	k_2^c (M ⁻¹ s ⁻¹)	ΔH^\ddagger (kJ·mol ⁻¹)	ΔS^\ddagger (J·mol ⁻¹ ·K ⁻¹)	ΔG^\ddagger_{df} (kJ·mol ⁻¹)	ΔG^\ddagger_{ef} (kJ·mol ⁻¹)
AN	$(1.28 \pm 0.04) \times 10^4$	$(3.8 \pm 0.5) \times 10^3$	$(2.6 \pm 0.4) \times 10^5$	32 ± 2^d	-65 ± 8^d	53.2 ± 0.4	42.6 ± 0.4
PC	$(1.70 \pm 0.05) \times 10^4$	$(1.6 \pm 0.2) \times 10^3$	$(6.9 \pm 0.3) \times 10^5$	54 ± 6^d	-5 ± 20^d	55.4 ± 0.3	
PC				35 ± 1^e	-16 ± 3^e		40.2 ± 0.1
AC	$(2.91 \pm 0.08) \times 10^4$	$(1.48 \pm 0.02) \times 10^4$		44 ± 1^d	-21 ± 2^d	49.8 ± 0.1	
PY	$(1.47 \pm 0.05) \times 10^3$	$(5.3 \pm 0.2) \times 10^2$	$(2.0 \pm 0.3) \times 10^4$	49 ± 4^d	-30 ± 10^d	58.1 ± 0.1	49.0 ± 0.4

^a See Table I for abbreviations. ^b $^{23}\text{Na}^+$ inverse lifetime for the two-site exchange (see eq 4). $[\text{NaBPh}_4] = 20 \text{ mM}$. $T = 301.5 \text{ K}$. $[\text{18C6}]/[\text{Na}^+] = 0.50$. ^c Obtained from eq 6. ^d Activation parameters of the unimolecular decomposition process (eq 1). ^e Activation parameters of the bimolecular exchange (eq 2). ^f ΔG^\ddagger is given at 301.5 K and calculated from k_{-1} and k_2 determined at this temperature.

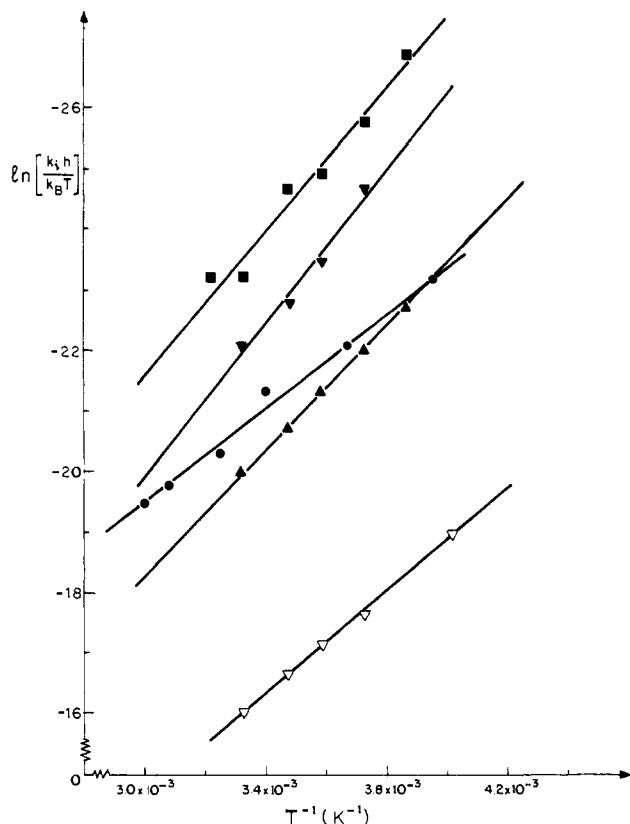


Figure 6. $(\ln k_i - \ln [k_B T/h])$ as a function of T^{-1} : (■), pyridine; (▼, ▽), propylene carbonate; (●), acetonitrile; (▲), acetone; (▽), $i = 2$, otherwise $i = -1$.

this approach, we assume that reliable $T_{2,ex}^{-1}$ data could be obtained when the exchange broadening is at least 20% of $T_{1,obs}^{-1}$. So, the limiting values of $k_A + k_B$ in Table I take into account not only the chemical shift difference but also the limitations on the experimental measurements.

Discussion

This study represents the first attempt at separating the two mechanistic contributions from the observed rate constant of dissociation of (18C6, Na^+). In acetone, the bimolecular contribution to the exchange is negligible, and the measured pseudo-first-order rate constant is directly related to the dissociation rate constant k_{-1} . The activation parameters which we determined are comparable to those published recently by Lincoln et al.:¹² $\Delta H^\ddagger = 44 \text{ kJ}\cdot\text{mol}^{-1}$ (Table II) as compared to $36 \text{ kJ}\cdot\text{mol}^{-1}$ ¹² and $\Delta S^\ddagger = -21 \text{ J}\cdot\text{K}^{-1}\cdot\text{mol}^{-1}$ as compared to $-17 \text{ J}\cdot\text{K}^{-1}\cdot\text{mol}^{-1}$.¹² The differences between the two results can be attributed primarily to the associated anion and probably to the differences in the sodium concentrations. In pyridine and acetonitrile, there is competition between the two mechanisms. Separation of the two components shows that the major contribution to the exchange is from the unimolecular dissociative mechanism. The reason why Lincoln et al.¹² observed spectra in the fast-exchange limit in acetonitrile is probably due to the nature and the concentration of the salt used in their study (NaSCN , 0.1 M). These conditions

would strongly favor the bimolecular exchange mechanism and speed up the exchange process. Strasser and Popov^{8b} have reported that the bimolecular exchange mechanism is operative in propylene carbonate. In confirming this, we found the system particularly interesting because it allowed the determination of the activation parameters for both mechanisms, with bimolecular exchange being the predominant one.

The enthalpy of activation for the unimolecular decomposition process follows the trend: $\text{AN} < \text{AC} < \text{PY} \approx \text{PC}$. This trend is opposite to what one would expect from a model based on the simple replacement of a sodium-ether oxygen bond by a sodium-solvent bond, without considering any other parameters. In such a simple model, an increase in the donicity number would lower the activation enthalpy. We have previously shown that the same opposite trend is seen in the values of the activation enthalpies of the dissociation of (DB18C6, Na^+) in several solvents.¹⁰ For example, in nitromethane, ΔH^\ddagger is $37 \text{ kJ}\cdot\text{mol}^{-1}$, and in dimethylformamide (DMF), ΔH^\ddagger is $51 \text{ kJ}\cdot\text{mol}^{-1}$. Clearly, the electron-donating ability of the solvent, as reflected by its donor number, cannot be directly related to the energetics of the dissociation process. Lincoln et al.¹² have also mentioned this for the (18C6, NaSCN) system. We have suggested that the plausible conformational rearrangements leading to the transition state are accompanied by partial desolvation of the complexed cation, reorganization of the solvent cage around the complex, and solvation of the partially decomplexed crown ether.¹⁰ Studies of the complexation reaction of 18-crown-6 with organic solvents, particularly acetonitrile and nitromethane, agree with this hypothesis.²⁷ There is also evidence for the coordination of the complexed sodium cation by at least one solvent molecule, since the relaxation rate of the complex is not linearly related to the viscosity of the solvent (see Table I). This would be the case if the electric field gradient were dependent only upon the crown ether oxygens and not on the solvent nature.²⁵ The ^{23}Na chemical shifts of (Na^+ , 18C6) span a much smaller range (from -16.3 ppm in NM to -12.4 ppm in PY) than the ones observed for (Na^+ , DB18C6) (from -16.0 ppm in NM to -7.8 ppm in PY).²⁸ This is indicative of the coordination of complexed Na^+ by fewer solvent molecules than for DB18C6.

The crystal structure of the (18C6, NaSCN) complex²⁹ shows a somewhat irregular pentagonal pyramidal coordination of Na^+ , resulting from the shift of one of the ethyleneoxy fragments in such a manner that the six $\text{Na}^+\cdots\text{O}$ distances are from 2.45 to 2.62 Å. An oxygen from a water molecule completes the coordination shell. The ^{23}Na parameters agree with a structure in solution that is similar to that of the crystal. In the case of pyridine, the very large quadrupolar coupling constant (T_1^{-1}/η

(26) Marcus, Y. J. *Solution Chem.* **1984**, *13*, 599-624.

(27) (a) Mosier-Boss, P. A.; Popov, A. I. *J. Am. Chem. Soc.* **1985**, *107*, 6168-6174. (b) Gold, H. S.; Rice, M. R. *Talanta* **1982**, *29*, 637-640.

(28) Lafleur, D. M.; Delville, A.; Maurice, L. J.; Detellier, C., to be published.

(29) (a) Dobler, M.; Dunitz, J. D.; Seiler, P. *Acta Crystallogr. Sect. B: Struct. Crystallogr. Cryst. Chem.* **1974**, *B30*, 2741-2743. (b) Dunitz, J. D.; Dobler, M.; Seiler, P.; Phizackerley, R. P. *Acta Crystallogr. Sect. B: Struct. Crystallogr. Cryst. Chem.* **1974**, *B30*, 2733-2738.

(30) (a) Izatt, R. M.; Terry, R. E.; Haymore, B. L.; Hansen, L. D.; Dalley, N. K.; Avondet, A. G.; Christensen, J. J. *J. Am. Chem. Soc.* **1976**, *98*, 7620-7626. (b) Michaux, G.; Reisse, J. *J. Am. Chem. Soc.* **1982**, *104*, 6895-6899. (c) Inoue, Y.; Hakushi, T. *J. Chem. Soc., Perkin Trans. 2* **1985**, 935-946.

= 145 Hz mP⁻¹ when $T_1^{-1}/\eta = 12$ Hz mP⁻¹ for PC) could be due to a distortion of the solvation shell by the bulky tetraphenylborate anion, in proximity of the complexed sodium, in a low dielectric solvent ($\epsilon = 12.9$).

The enthalpy-entropy compensation effect that we have observed and discussed in the case of (DB18C6, Na⁺) is also operative for (18C6, Na⁺). The same effect is well documented for thermodynamic data.³⁰

For the bimolecular mechanism, ΔG^* varies in the order PC < AN < PY. This trend suggests that the major contribution to the exchange barrier is the desolvation of the incoming cation.

Despite the differences in the rigidity of the ligand, in the basicity of the ether oxygens, and in the structure of the complexes in solution, there is a remarkable similarity between the activation parameters for the dissociation of (DB18C6, Na⁺)¹⁰ and (18C6, Na⁺) in acetonitrile. Direct comparison is possible since the unimolecular exchange rates were obtained under similar experimental conditions. ΔG_{300K}^* is 53 kJ·mol⁻¹ for both systems.

The lower enthalpy of activation for (18C6, Na⁺) is compensated for by a lower entropy of activation. The more flexible 18C6 gives rise to a lower activation enthalpy. The fact that the activation parameters for both systems are comparable is another indication of the role of the solvent in the barrier of dissociation.

Conclusion

In the four nonaqueous solvents of this study, the sodium cation exchanges between solvated and 1:1 complexed sites when it is in the presence of 18-crown-6. The exchange follows two mechanisms which are competitive. The determination of the pseudo-first-order rate constants for the exchange for various concentrations and temperatures allows the separation of both contributions to the exchange. In favorable cases, such as propylene carbonate, it is possible to determine the activation enthalpy and entropy for both processes. The mechanism is almost exclusively unimolecular in acetone. In pyridine, acetonitrile, and propylene carbonate, both mechanisms are in competition. Our results show that the unimolecular decomplexation is the product of several factors, the least of which is not the role of the solvent. In general, there is a compensation effect for the enthalpy and the entropy of activation. In particular, this effect is at the origin of the identical free energy of activation for (18C6, Na⁺) and (DB18C6, Na⁺) in acetonitrile.

Acknowledgment. The Natural Sciences and Engineering Research Council of Canada (NSERCC) is acknowledged for financial support.

Registry No. Na, 7440-23-5; (18-crown-6, Na⁺), 31270-12-9.

Is Bound CO Linear or Bent in Heme Proteins? Evidence from Resonance Raman and Infrared Spectroscopic Data

Xiao-Yuan Li and Thomas G. Spiro*

Contribution from the Department of Chemistry, Princeton University, Princeton, New Jersey 08544. Received July 22, 1987

Abstract: The vibrational data on heme-CO complexes are analyzed with a view toward elucidating the structural evidence for distorted FeCO units in heme proteins. The effects of FeCO distortion on the vibrational frequencies are attributable to back-bonding changes, as evidenced by the correlation of ν_{FeC} with ν_{CO} . Steric restraint of perpendicular binding increases Fe → CO back-donation slightly. This is opposite to the direction expected if the FeCO unit is bent but is consistent with the expected effect of two other distortion coordinates, FeCO tilting and porphyrin buckling. Larger effects on back-bonding are attributable to polar interactions of distal residues with the bound CO, especially H bonding. Substantial FeCO bending is inconsistent with the relatively small frequency separation between ν_{FeC} and δ_{FeCO} observed in all adducts so far examined; this separation is calculated to increase strongly with the bending angle due to mixing of the modes. For a given displacement of the O atom from the heme normal, the energy required for the three distortion coordinates is calculated to increase in the order tilting < buckling < bending. The energy is minimized, as are the individual angular displacements, if all three contribute to the actual molecular distortion, and the small net change may result from the opposing effects of bending and of tilting and buckling in ν_{FeC} . This concerted model of FeCO distortion is not inconsistent with the available X-ray crystal structure data. It is inconsistent with EXAFS analysis of MbCO at 4 K, which has yielded a small value, $127 \pm 4^\circ$, for the FeCO angle from the attenuation of second-shell scattering relative to a protein-free model. This attenuation might be due instead to other changes in second-shell scattering, e.g. due to porphyrin buckling.

Introduction

X-ray and neutron scattering crystal structures are available for the carbon monoxide adducts of several heme proteins.¹ An interesting observation is that nonbonded contacts in the heme pocket frequently prevent the bound CO from adopting its expected configuration, namely a linear FeCO unit normal to the

heme plane. This structure, established crystallographically for several protein-free CO adducts of iron(II) porphyrins,² is the one expected from considerations of maximum orbital overlap in the well-established π back-donation bonding model for transition-metal carbonyls. Deviations from this geometry are expected to cost energy, and it has been suggested by Collman and co-workers³ that the steric hindrance seen in heme proteins may play a functional role in lowering the CO affinity, thereby raising the threshold for CO poisoning. Whether the CO affinity is actually

(1) (a) Kuriyan, J.; Wiltz, S.; Karplus, M.; Petsko, G. *J. Mol. Biol.* **1986**, *192*, 133-154. (b) Hanson, J. C.; Schoenborn, B. P. *J. Mol. Biol.* **1981**, *153*, 117. (c) Baldwin, J. M.; Chothia, C. *J. Mol. Biol.* **1979**, *129*, 175. (d) Baldwin, J. M. *J. Mol. Biol.* **1980**, *136*, 103. (e) Steigeman, W.; Weber, E. *J. Mol. Biol.* **1979**, *127*, 309. (f) Tucker, P. W.; Philipps, S. E. V.; Perutz, M. F.; Houtchens, R. A.; Caughey, W. S. *Proc. Natl. Acad. Sci. U.S.A.* **1978**, *75*, 1076. (g) Heidner, E. J.; Ladner, R. C.; Perutz, M. F. *J. Mol. Biol.* **1976**, *104*, 707. (h) Norvell, J. C.; Nunes, A. C.; Schoenborn, B. P. *Science (Washington, D.C.)* **1975**, *190*, 568. (i) Padlan, E. A.; Love, W. E. *J. Biol. Chem.* **1974**, *249*, 4067. (j) Huber, R.; Epp, O.; Formanek, H. *J. Mol. Biol.* **1970**, *52*, 349.

(2) (a) Peng, S. M.; Ibers, J. A. *J. Am. Chem. Soc.* **1976**, *98*, 8032. (b) Scheidt, W. R.; Haller, K. J.; Fons, M.; Fashiko, T.; Reed, C. A. *Biochemistry* **1981**, *20*, 3653. (c) Caron, C.; Mitschler, A.; Riviere, G.; Ricard, L.; Schappacher, M.; Weiss, R. *J. Am. Chem. Soc.* **1979**, *101*, 7401.

(3) (a) Collman, J. P.; Brauman, J. I.; Halbert, T. R.; Suslick, K. S. *Proc. Natl. Acad. Sci. U.S.A.* **1976**, *73*, 3333. (b) Collman, J. P.; Brauman, J. I.; Everson, B. L.; Sessler, J. L.; Morris, R. M.; Gibson, Q. H. *J. Am. Chem. Soc.* **1983**, *105*, 3052.